# THERMAL MODELING AND DESIGN OF A MICRO-ROVER FOR LUNAR POLAR EXPLORATION

Virtual Conference 19–23 October 2020

Paulo R.M. Fisch1, Jasmine M. Bitanga2, William L. Whittaker3

[1]Robotics Institute, Carnegie Mellon University, 5000 Forbes Ave, Pittsburgh, PA 15213, USA, E-Mail: paulo.zazo@gmail.com

[21]Robotics Institute, Carnegie Mellon University, 5000 Forbes Ave, Pittsburgh, PA 15213, USA, E-Mail: jbitanga@andrew.cmu.edu

[31]Robotics Institute, Carnegie Mellon University, 5000 Forbes Ave, Pittsburgh, PA 15213, USA, E-Mail: red@cmu.edu

## ABSTRACT

MoonRanger is an autonomous micro-rover that will explore the south pole of the Moon for lunar ice in 2022. It will fly aboard the Masten XL-1 lander on a Commercial Lunar Payload Services (CLPS) mission. The cryogenic cold of a shadowed pole is challenging for any rover. This is vastly more so for a micro-rover that lacks the thermal inertia and regulation capabilities of its larger counterparts. This paper details the thermal design, modeling, and analysis of MoonRanger. It also assesses the validation of the viability of the thermal control of micro-rovers at the lunar poles for future missions.

## 1. INTRODUCTION

Planetary rovers are historically large, controlled by human operators, isotope-powered and slow. MoonRanger presents a major paradigm shift from that generation of rovers. It is fast, autonomous, solar-powered, and small. Those characteristics create major challenges for thermal regulation during its mission to the lunar south pole in 2022, where harsh environmental conditions accentuate those hardships.

Ice deposits have the potential to supply human expeditions to the Moon with water and oxygen, and to provide propellants to fuel expeditions to deep space [1]. The viability of that vision is dependent on the extent to which ice is accessible and concentrated, as well as the rover's feasibility to detect ice at various depths. Ice is present at the lunar poles partly because of their cryogenic surface temperatures, which vary between 50K and 200K [2].

Surface temperatures constitute only part of the challenge in achieving a viable thermal design for a micro-rover. During cislunar transit, the rover is alternately exposed to darkness and to direct sunlight. Additionally, low grazing angles of polar sun incidence present notable differences versus the high sun angles experienced by low-latitude rovers.

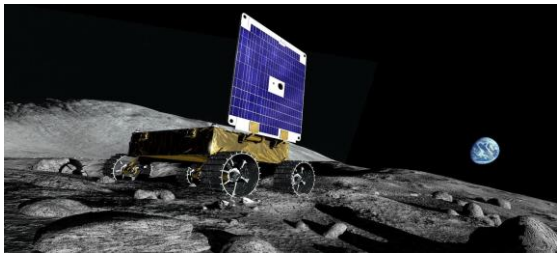

*Figure 1. Artistic illustration of MoonRanger Source: Mark Maxwell*

Moreover, the rover's thermal conditions are strongly dependent on its position relative to the sun, which directly impacts autonomy and route planning. Fig. 2 shows a top-down view of the reference frame for azimuth angles ($\boldsymbol{\varphi}$) and a side view for elevation angles ($\boldsymbol{\theta}$). Notice that on the poles, higher elevation angles are caused by slopes rather than by the lunar movement around the sun, since the Moon has a rotation tilt close to zero, resulting in sunlight nearly parallel to the ground throughout the year.

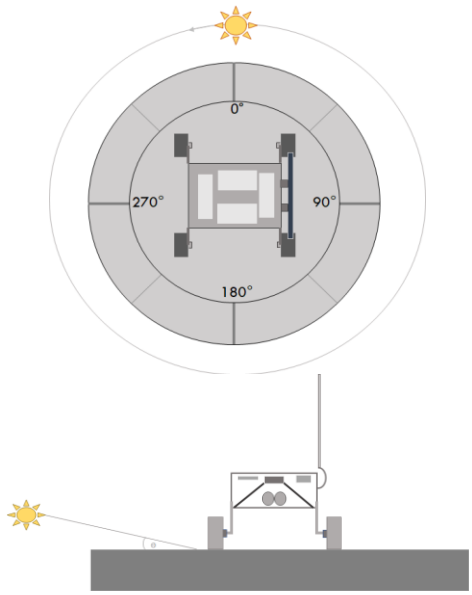


*Figure 2: Reference frame centered on the rover*

## 2. THERMAL DESIGN PHILOSOPHY

MoonRanger employs a plethora of both passive and active thermal solutions. Most of the passive protection devices function by optimizing optical properties of the rover`s surfaces [4][5]. Some of these solutions include the application of a low-absorptivity, high-emissivity finish on the solar panel, Vapor Deposit Aluminum tape on the inside of the chassis to mitigate radiative interactions, and a low-absorptivity, high-emissivity film on the radiator for optimized heat rejection.

On the radiator, localized finishes, such as VDA tape or white paint tailor optical properties for the heat rejection needs of each component. Some solutions also use low-conductivity interfaces, such as PEEK interfaces between motors and wheels to increase thermal resistance and mitigate heat losses via conduction to lunar regolith.

The active thermal control system uses heaters and an on/off logic to provide heat to vital components in case these drop below a threshold chosen for each individual component. Heaters are located in every internal avionics component, wheel motors, external lasers and sun sensors.

Sensitive avionics are required to have margins from their minimum and maximum operating temperatures.With this margin philosophy, all internal components must be within the highest component temperature for cold operation and the lowest component temperature for hot operation. Therefore, the temperature range for surface operations is from -10°C to 35°C. For transit, the range lies between -15°C and 40°C.

## 3. THERMAL RESISTANCE NETWORK

A simplistic early model for identification of cases that gave out hottest and coldest inner temperatures considered an enclosed chassis, an upright solar panel, and an infinite regolith plane. Conduction between elements was considered only on the radiator, whose thickness and conductivity create a relevant thermal resistance. The only heat transfer mechanism between other nodes on the resistance network was radiation. Each exterior node had an assigned solar absorptivity and emissivity, which then dictated the radiative interactions between surfaces. Multilayer Insulation (MLI) was modeled as present on every surface of the chassis other than the radiator. Thermal sources and sinks for this model included direct sunlight, reradiation from surrounding regolith, dissipation from avionics, and radiation to space at 3K. Fig. 3 shows a schematic of this model.

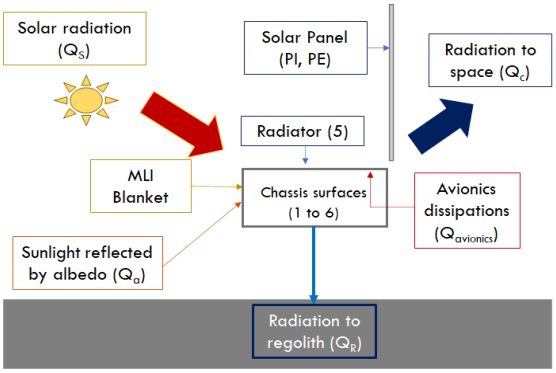


*Figure 3: Thermal Resistance Network had major simplifications*

For this initial analysis, the main parameters were avionics dissipation, number of MLI Layers, regolith temperature, and elevation angle. Dissipations assumed were 37.5W and 52W from early lowest and highest power consumption estimates. Regolith temperatures were 80K, 120K and 150K. The MLI had its first and second surfaces with ε=0.5 with 25 and 30 layers. Azimuth angles varied from 0° to 360° in 45° steps, while elevation angles varied from 0° to 15° in 5° steps. The radiator had uniform optical properties, with emissivity equal to 0.76 and an absorptivity of 0.14.

With the objective of keeping simulation simple for better understanding of the system's thermal behavior, the thermal resistance network considered steady-state solutions for surface operations only. After running all possible combinations of parameters, it was possible to identify a hot case and a cold case. The hottest temperatures were observed with 30 layers of MLI, 52W of dissipation, 150K regolith temperature, 270° azimuth and 15° elevation. The coldest conditions were found with 25 layers of MLI, 37.5W of dissipation, 80K regolith temperature, 0° azimuth and 0° elevation. Fig. 4 and Fig. 5 show the internal radiator and average internal temperatures for both conditions.

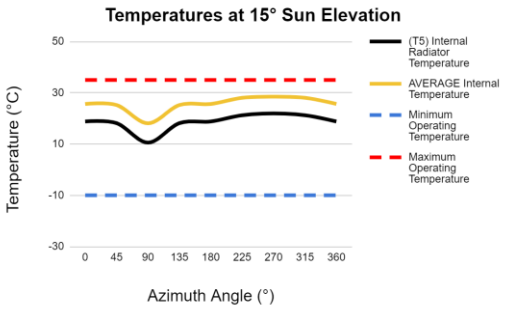


*Figure 4: Hottest case is at* $\boldsymbol{\varphi}$*=270°* $\boldsymbol{\theta}$=15°

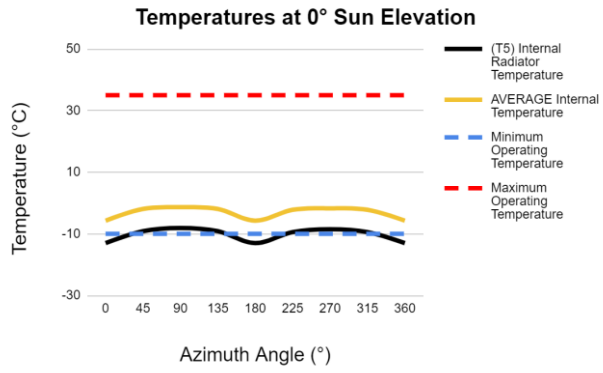


*Figure 5: Figure 4: Coldest case is at* $\boldsymbol{\varphi}$*=0°* $\boldsymbol{\theta}$=0°

Some characteristics of the system could also be observed with the Thermal Resistance Network. At higher elevation angles, the shadow casted by the solar array into the radiator at 90° azimuth lowers the internal temperatures. At lower elevations, those dips in temperature happen at 0° and 180° azimuth, where sunlight runs parallel to the solar array. Those results served as a baseline for further investigation with higher fidelity models.

## 4. FINITE ELEMENT MODEL

The Finite Element Model was developed in the ANSYS Mechanical APDL environment. It included some details which were omitted in the Thermal Resistance Network. Chief among those are the inclusion of separate avionics, which were initially considered as a heat input on the radiator, which had uniform emissivity and absorptivity. Wheels and wheel brackets were included, as well as solar panel hinges connecting the chassis and the solar panel. Fig. 6 shows the mesh used for simulations.

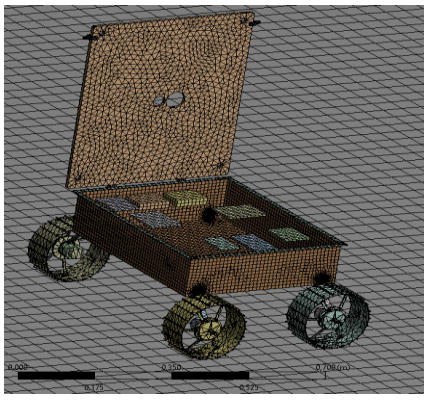

*Figure 6: Finite Element Model Mesh*

The mesh had 73040 elements and 230517 nodes. It helped to identify more nuanced thermal behaviors in the system, such as hot and cold spots on the radiator caused by the central computer and other components. Conduction from the wheels to regolith presented a large heat sink which was not considered in the Thermal Resistance network.

Ansys enabled the inclusion of multiple parameters to the model, such as the thermal conductivity of a multitude of materials, such as carbon fiber, 7075 Aluminum or Stainless steel. However, the CAD model from which the mesh was generated still included multiple simplifications; no bolts or bonding materials were included. Avionics components were modeled as solid bricks with uniform volumetric heat generation. No internal structural elements were included.

Some of those simplifications come from software limitations. The largest hindrance of the Finite Element Model is that ANSYS is not the standard for the thermal analysis of space systems. A main constraint is radiation solving and surface contact input methods. More specifically, heat fluxes from sunlight must be calculated individually, which hinders the fidelity with respect to lighting. Moreover, contact between surfaces is not optimized for space applications and makes modeling of bonding materials more difficult.

The ultimate purpose of the Finite Element Model was to introduce more detail and check for agreement with the Thermal Resistance network. All simulations on the Finite Element Model were steady-state simulations. Fig. 7 shows the result of a simulation for the hottest condition.

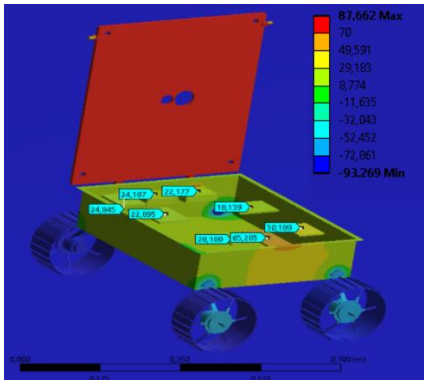


*Figure 7: Simulation results for hot case on FEM show large hot spot on central computer*

This model identifies a hot spot on the central computer (in orange), reaching a temperature of about 65°C. The central computer dissipates about 20W in the form of heat as it operates, concentrating heat rejection in a smaller section of the radiator. As a result, other avionics components with smaller dissipations achieve lower temperatures.

It is also important to point out that the colder temperatures on the lower corners of the chassis identify a potent heat sink on the wheels touching the regolith.

Comparing FEM and Thermal Resistance Network results, temperatures agreed with discrepancies of up to 4%. This indicates the systems behave similarly in steady-state condition. Table 1 compares both results.

| Component | TRD (K) | FEM (K) | Discrepancy |
|---|---|---|---|
| Avionics | 271.1 | 264.1 | 2.6% |
| Radiator | 270.5 | 259.7 | 4.0% |
| Solar Panel Interior | 353.6 | 358.5 | 1.4% |
| Solar Panel Exterior | 355.2 | 360.8 | 1.5% |

*Table 1: Thermal Resistance Network and Finite Element Model show agreement on results*

These results showed an agreement between both models and showed some points of interest that were carried to the next models. Some of those considerations include the identification of heat sinks on the wheels, conduction from the solar panel to the chassis, and the localization of hot and cold spots on the radiator.

## 5. FINITE DIFFERENCE MODEL

As the design progressed, the team developed a Finite Difference Model in Thermal Desktop, the standard software for thermal design of space systems. It enabled increased fidelity concerning optical and thermal properties of materials. The radiator had different optical properties in each region, according to the heat rejection needs of each avionics component. Refinements in modeling of heaters, heat sources and sinks were also included in this model.

Thermal Desktop also improved simulation fidelity by enabling the creation of orbits. The software calculates heat sources and sinks automatically to every surface assigned to a given orbit. Some sources and sinks include sunlight, infrared planetshine, light reflected by a celestial body's albedo, radiation to space, among others. In previous models, radiation from celestial bodies had to be calculated separately and then input on the software for each orbital condition.

For the sake of simplicity, internal avionics are divided into two groups; Red and Green avionics. Green-group avionics are closer to the solar array hinges and are consequently more affected by the variation in chassis temperature those components cause. On the other hand, Red-group avionics are located further from the solar array hinges, which causes them to present less temperature variation. Figure 8 shows the components and their respective groups.

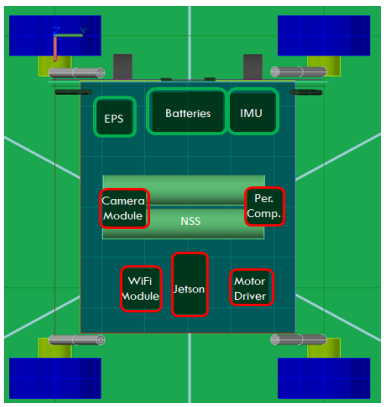


*Figure 8: Red and Green avionics groups*

### 5.1. Transit Model

The Transit Model simulated MoonRanger on the path between Earth and the Moon. The rover was attached to the lander via a Hold Down and Release Mechanism. Its solar panel was in the stowed configuration. Figure 9 shows the transit model.

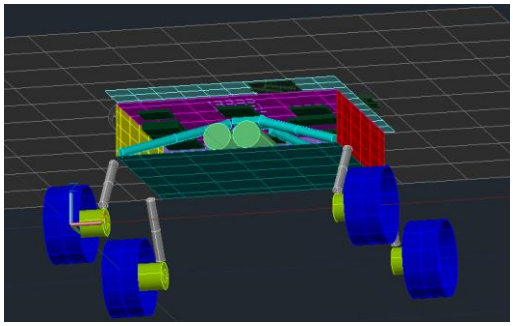

*Figure 9: Finite Difference model in transit configuration*

This model had 863 nodes, 26 surfaces, 53 finite difference solids, 28 contactors and 100 conductors. Convergence criteria were 100 maximum transient iterations, 0.001°C maximum temperature change and a Bij/Fij cutoff factor of 0.001.

This model also included heaters to internal avionics components and wheel motors. Power to those heaters will be provided by the lander during flight, so this analysis sets the requirement for power provided by the lander. This analysis considers 10W total to the heaters. In section 5.4., a power analysis details the choice of this value.

### 5.1.1. Cislunar Transit

During cislunar transit, the rover can be exposed to complete darkness or direct sunlight, providing two greatly distinct and extreme conditions. Firstly, survival at complete darkness was evaluated, with 10W provided to heaters coming from the lander. All components had an initial temperature of 20°C. Figure 10 shows a schematic of the model for complete darkness.

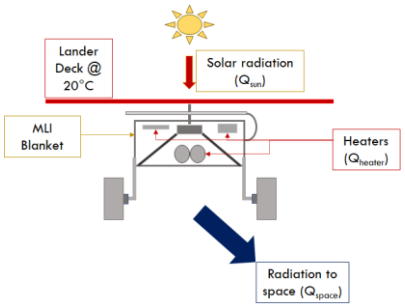


*Figure 10: Schematic of transit model in complete darkness*

In this configuration, the lander deck shadowed the rover from the sun completely. The lander deck was assumed to be at a constant 20°C and radiation to space considered a background temperature of 3K.

Figures 11 and 12 show the temperature distribution across the model and its transient response, respectively.

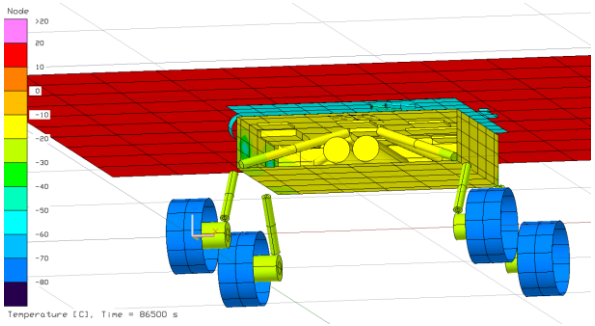


*Figure 11: Temperatures during cislunar transit demonstrate survival throughout the mission*

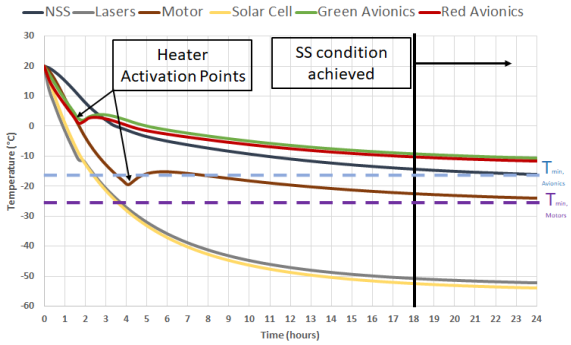


*Figure 12: Steady state is reached after 19 hours with heaters activated*

Internal avionics remained above the lowest temperature acceptable (-15°C) for storage considering a 15°C margin from the highest cold storage temperature throughout the simulation.

Steady state was achieved after about 19 hours, when temperatures between timesteps varied less than 0.1°C for every component.

The lack of a sawtooth oscillation pattern on components with heaters indicate the heaters are activated when steady state conditions are reached.

### 5.1.2. Surface Operations Model

The Surface Operations Model simulated MoonRanger while operating on the lunar surface after release from the lander and deployment of the solar panel. This is the configuration MoonRanger will have until the end of the mission.

Compared to transit, surface operation introduces some heat sinks, such as conduction to lunar regolith and a stronger effect from light reflected by albedo. Additionally, avionics are operational during this stage of the mission, adding dissipations as a heat source. Figure 13 shows the heat sources and sinks for this condition, while Figure 14 shows the Surface Operations Model.

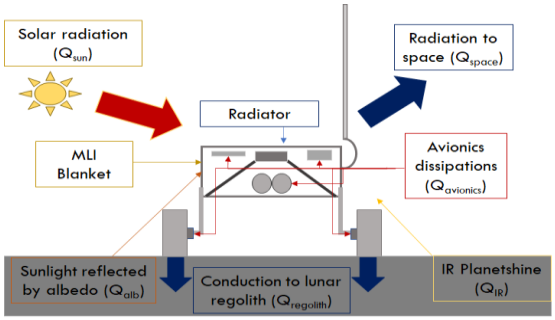


*Figure 13: Heat sources and sinks for surface operations*

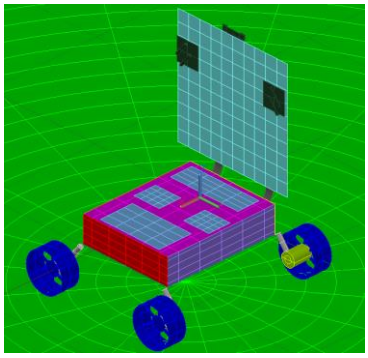

*Figure 14: Surface Operations model*

This model had 1542 nodes, 25 surfaces, 60 finite difference solids, 31 contactors and 100 conductors. Convergence criteria were 100 maximum transient iterations, 0.001°C maximum temperature change and a Bij/Fij cutoff factor of 0.001.

It also considers the individual dissipations of avionics, motors and sensors. These values vary according to the rover's operational regime.

### 5.1.3. Hot Case

The hottest condition MoonRanger will face on the lunar surface is at 270° azimuth and 15° elevation. This would be a situation in which the rover is at a slope, causing the rover to be tilted relative to the low-grazing sunlight and illuminating the radiator. Figure 20 shows the lighting conditions for this simulation.

This condition also considers the largest power draw possible, caused by hazardous terrain and high computational demand. Total power draw in this condition is 51W, with the rover starting the simulation at 20°C and the lunar surface at 200K (-73.15°C).

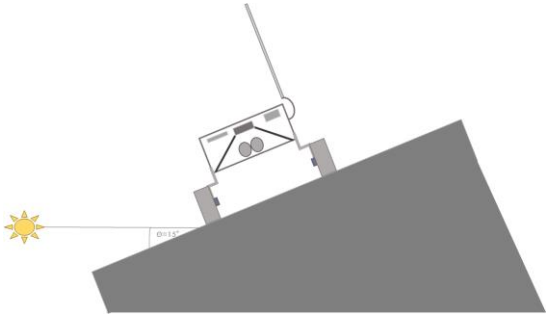

*Figure 15: Sun elevation on hot case is caused by slope rather than by orbital dynamics*

At the end of this simulation, all internal avionics were below the 35°C threshold when the system reached steady-state conditions. The white coating on the solar array rejects heat efficiently and absorbs less heat from sunlight than the bare carbon fiber finish of the solar panel, keeping it within about 20°C. Some oscillation is present at the solar array, indicating numerical fluctuations caused by mesh coarseness. Figure 16 shows the temperature distribution across the rover and figure 17 displays the transient response throughout the simulation.

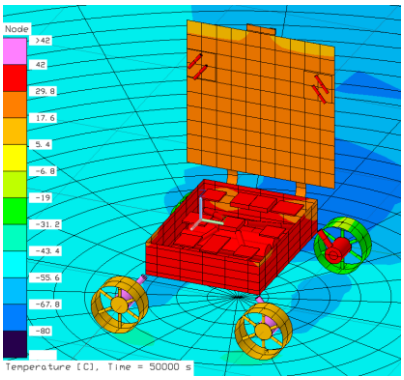


*Figure 16: MoonRanger's shadow on lunar soil causes cold spots*

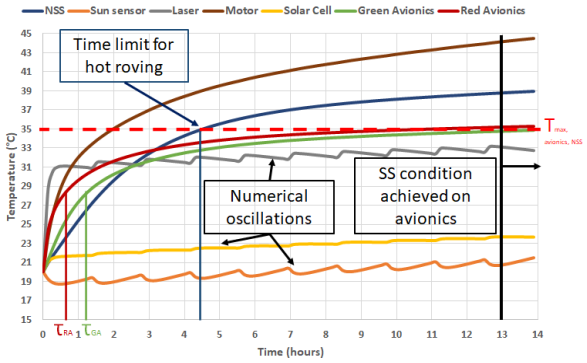


*Figure 17: Internal avionics fulfill their temperature requirements during hottest operation conditions*

From the graph, it is possible to obtain the time constant of some components as dynamic systems. Red-group avionics components have a time constant of about 45 minutes, while their Green-group counterparts' time constant is of about 1 hour and 15 minutes. The NSS with its larger thermal inertia has a time constant of nearly 2 hours and 45 minutes.

Under this condition, the NSS' temperature goes above its limit of 35°C after circa four and a half hours. Other internal avionics components stay beneath 35°C in steady-state regime. Motors do not reach steady-state during this simulation.

### 5.1.4. Roving In Complete Darkness

Since one of MoonRanger's mission objectives is to search for ice at the lunar south pole, it will have to endure cryogenic permadark conditions for extended

periods of time, as those conditions are the most likely to support ice on the moon. The rover starts the simulation at 20°C, while the regolith starts at 50K (-223.15°C), which is the predicted temperature by Park et. al. [2]. This simulation also considers no light reflected by the lunar surface reaches the rover.

This simulation considers a total of 40W dissipation from avionics and motors. A total 12W of heaters on internal avionics, a total 2W on lasers, 2W total on sun sensors, and 3W total to wheel motors were available in case any component required it. Figure 18 shows the temperature distribution across the model and Figure 19 displays the transient response.

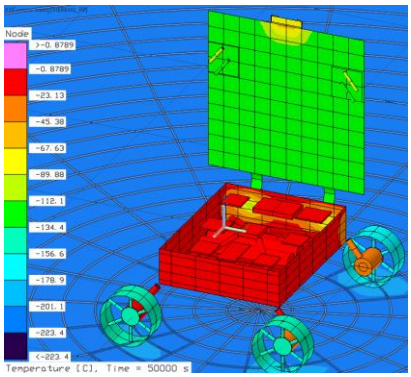


*Figure 18: Solar panel cools significantly under permadark conditions*

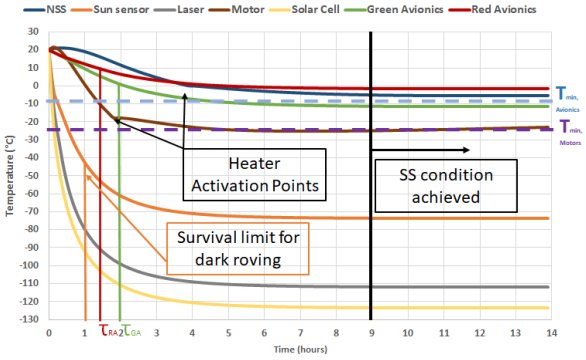


*Figure 19: 1 hour is the limit for dark roving*

From the graph, the time constant of the Green-group avionics is of about 1 hour and 15 minutes, while its Red-group counterparts have a time constant of about 2 hours. Motor heaters activate after about 1 hour and 45 minutes, NSS heaters activate after about 3 hours and 45 minutes. Laser and sun sensor heaters activate after less than 10 minutes.

Using 40W dissipation and about 8W for heaters, the rover can maintain its internal avionics above -10°C under steady-state condition. Motors also remain above -25°C under steady-state condition. The limiting factor for roving in permadark regions is the sun sensors and lasers. These components drop below their cold soak temperatures after about one hour. After this time, these components risk being damaged.

### 5.2. MLI Analysis

Two MLI analyses were carried out: One during cislunar transit and another for surface operations. Cislunar transit considers the same conditions as in section 5.1.1. Power supplied by the lander amounts to 10W. Figure 20 shows the temperature of critical components varying with the MLI's effective emissivity [6] during cislunar transit.

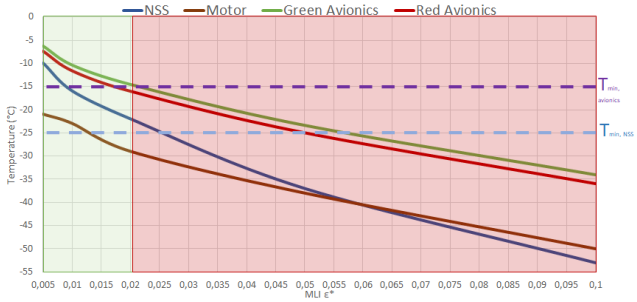


*Figure 20: Transit requires low ε**

It can be seen the NSS is a limiting component and that it is more sensitive to changes on the MLI's effective emissivity, as it is assembled directly on the chassis' belly, which is directly exposed to space. It can also be noticed that temperatures drop as the effective emissivity increases, since a larger ε* means more radiative heat loss to space. Therefore, every ε* value below 0.025 enables survival during cislunar transit.

The surface operations analysis considers the same conditions than those of sections 5.2.1 and 5.2.2. Figure 21 displays the temperature of critical components varying with MLI's effective emissivity during surface operations for the hottest and coldest case.

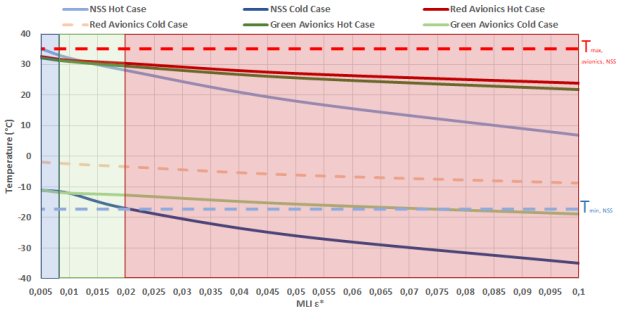


*Figure 21: Surface operations have an ideal gap for ε**

It is possible to see from the graph that the NSS is also the component most sensitive to MLI ε* variation during surface ops. The gap between Green and Red avionics is larger for the cold case than for the hot case. Consequently, the acceptable range for Surface Ops is the limiting factor to the choice of MLI ε* and determines the acceptable range as being 0.007< ε*<0.02.

### 5.3. Power Analysis

Given cislunar transit is the limiting condition for transit, a power analysis with MoonRanger's design is carried out to investigate how much power needs to be provided to the rover's heaters and ensure survivability for transit. The conditions are the same as detailed in section 1.1 with MLI ε* = 0.01. Power input varies from 8W to 14W. Results are displayed by Figure 22:

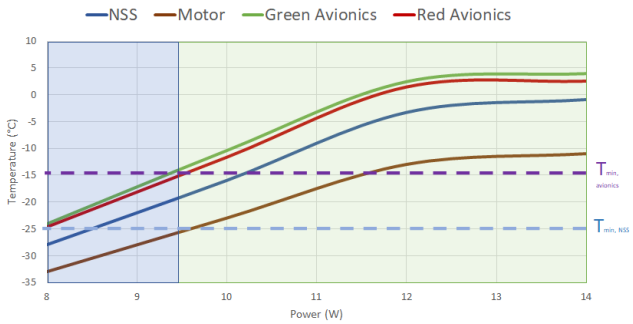


*Figure 22: 9.5W is the minimum for surviving transit in complete darkness*

Results show the minimum power required to keep temperatures within storage temperature range (i.e. avionics above -15°C and NSS above -25°C) is 9.5W. It can also be noticed that the temperature's growth rate changes from 12W onwards, indicating an increase in power from that value on the power can keep the system oscillating between the temperatures set for the active control system during transit.

## 6. THERMAL IMPACT ON AUTONOMY

Thermal regulation has a great impact on autonomy, especially concerning a hostile environment, such as the lunar south pole. It can imply on the rover stopping for a period of time for cooling when exposed to hot conditions, much like it can freeze and have some components damaged due to cold-soak in permadark environments. Consequently, these considerations need to be included on the autonomy algorithm that commands the rover during the mission. Given the strong dependency between thermal conditions and solar positioning, maneuvers changing solar orientation can be preprogrammed. For example, a quick change from 90° azimuth to 0° azimuth can be used as a "cooling route.

An advantage MoonRanger possesses compared to other planetary rovers is its sizable power-richness. It generates about 70W from solar power, while consuming at most 50W when exposed to sunlight. Therefore, it can operate for extended periods of time, increasing its range, also enabling longer periods of time under permadark conditions.

## 7. CONCLUSION.

This paper demonstrated the thermal solutions and design process for MoonRanger. The team also obtained gradual increase in model fidelity throughout the project, coming from a Thermal Resistance Network, evolving to a Finite Element Model, which led to the Finite Difference Model, the gold standard of space systems thermal design. Finally, this high fidelity model verified survivability through multiple mission phases, identifying extreme cases. Temperature-sensitive components remained within their operational ranges with margin. MoonRanger is a pioneer for cold planetary body micro-rovers. Its thermal regulation technologies will set the standard for future missions and demonstrate the feasibility of autonomous micro-roving under unforgiving conditions, such as those found on the lunar south pole.

**Acknowledgement**

The technology, rover development and flight are supported by NASA LSITP contract 80MSFC20C0008 MoonRanger

**References**

[1] M. A. Siegler et. al. (2018) *Subsurface Ice Stability on the Moon* Abstract #5038.

[2] T.Y. Park et. al. (2018) *Preliminary Thermal Design and Analysis of Lunar Lander for Night Survival*. International Journal of Aerospace Engineering. DOI 10.1155/2018/4236396

[3] Sapunkov, O. et. al. (2019) *Passive Thermal Analysis and Regulation for a Lightweight Lunar CubeRover*

[4] Gilmore, D.G. (2002) *Spacecraft Thermal Control Handbook.*

[5] Kauder,L. (2005) *Spacecraft Thermal Control Coatings References, NASA/TP-2005-212792*.

[6] Finckenor, M.M. and Dooling, D. (1999) *Multilayer Insulation Material Guidelines, NASA/TP-1999-209263*.